

Effects of plaster to water ratio on physical and mechanical properties of ceramic pieces produced by the slip casting process

L. B. Palhares¹, D. F. Galvão^{1}, P. R. P. de Paiva¹*

¹Federal Center for Technological Education of Minas Gerais, Department of Materials Engineering, Belo Horizonte, MG, Brazil

Abstract

In the slip casting process, the relationship between the amount of plaster and water used in the production of molds influences the production of ceramic materials, because the higher the water content in the mixture, the lower the mechanical strength of the mold and higher the water absorption rate. In order to evaluate the influence of the variation in the plaster/water (P/W) ratio in the production of ceramic pieces, plaster molds with P/W ratios of 2.0, 1.67, 1.43, and 1.25 (100 parts of plaster/50, 60, 70, and 80 parts of water by weight) were manufactured and used in the production of ceramic pieces. It was found that the fluidity, density, flexural and compressive strength of the molds decreased with the increase of water content. For pieces sintered at 1050 °C, higher density and lower porosity were observed for ceramic materials obtained with molds with higher plaster/water ratios.

Keywords: slip casting, plaster molds, characterization.

INTRODUCTION

Slip casting is a simple and traditional process, which can be applied to the production of regular or advanced ceramic pieces with hollow, solid, or even complex profiles. The process consists of preparing a stable suspension of a ceramic powder in either an aqueous or non-aqueous liquid, which is then transferred into a porous plaster mold [1]. The porous structure of the plaster molds is decisive in defining the properties and structure of the pieces obtained by slip casting [2]. An important objective of the ceramic processes consists of attaining green bodies with homogeneous microstructures, as they affect the piece's behavior at the sintering stage, as well as its physical and mechanical properties [3]. Plaster is a fragile, porous material, of easy molding and low cost, being the most used material on slip casting for mold production. According to Barbosa et al. [2], 3% of plaster production in Brazil (approximately 100 thousand tons) is applied to the ceramic industry in the form of molds. In Brazil, 95% of plaster production is concentrated in the state of Pernambuco. About 96% of the produced material is destined directly to civil construction as foundry and coating plasters for the production of slabs, blocks, and wall coverings. A more pure version, known as industrial plaster, is used in the manufacture of ceramics, porcelain, and as raw material in the glass industries [2]. The plaster is a hemihydrate calcium sulfate of chemical formula $\text{CaSO}_4 \cdot 0.5\text{H}_2\text{O}$, produced by calcining the gibbsite at temperatures between 120 and 160 °C, through the reaction [4]:



When plaster and water are mixed, the reverse reaction A takes place, and the water is reabsorbed, reforming the gibbsite. The reaction is exothermic and results in a solid with needle-like crystals entwined. Stoichiometrically, only 18.6% by weight of water is needed for the reaction to occur, but in practice excess water is used, leading to considerable porosities after the molds have dried [4]. The morphology of the crystals formed depends on the variation of hydration conditions. Due to the possibility of varying parameters at each stage of the process (dissolution, nucleation, and growth of hemihydrate crystals), different microstructures can be obtained, with larger and irregular crystals reducing the density and mechanical strength of the plaster due to their greater porosity, while smaller prismatic crystals allow greater compaction [2]. Plaster is a fundamental material in the slip casting process. Its special properties allow the construction of porous molds, which enable duplicating complex models, providing final products with all and any desired details. The pores in the mold create a suction pressure due to surface tension forces and cause the liquid to be removed from the suspension. The casting rate is determined partially by the mold's permeability. This is mainly affected by the plaster/water ratio in the initial mixture, as well as by the amount of water in the mold before use (drying). A uniform and homogeneous product are possible only if the initial particle suspension has high homogeneity and stability. The quantity of water at the plaster influences the porosity and the absorption velocity of water from suspension (the casting rate). As bigger as the quantity of water, bigger is the porosity and the casting rate. This homogeneity must be preserved during all the processing steps, as follows: slip casting, drying, heating, and sintering [3].

For this paper, residues generated in the slate extraction were used for the production of the ceramic pieces. The

*douglasfilipe_cpm@hotmail.com

<https://orcid.org/0000-0001-9699-6540>

use of waste as an alternative raw material may reduce the environmental impact generated by the slate's production process, in addition to promoting the appearance of new work and income opportunities. According to Ribeiro *et al.* [5], it is estimated that the amount of waste generated by the processing of ornamental rocks can reach 40% to 60% of the total global production. Considering the production of waste was 50% of the total volume of processed natural rocks in 2019 in Brazil, which produced approximately 9 million tons of ornamental stones [6], about 4.5 million tons of waste was generated. Such residues have the potential to be employed as raw materials in manufacturing ceramic pieces through slip casting. In this context, the objective was to evaluate the influence of the plaster/water ratio (P/W) on the physical and mechanical properties of the produced pieces. Determining the consistency of the most suitable plaster mold for the piece manufacturing via slip casting process can lead to an optimization of the mold properties, increasing its lifespan, reducing the residue generation after the process, and decreasing the companies' expenses.

MATERIALS AND METHODS

The commercial plaster powder was obtained from Aciflex do Brasil. Plaster molds were made using different plaster/water (P/W) ratios of 50, 60, 70, and 80 (100 parts of gypsum/50, 60, 70, and 80 parts of water by weight). The plaster was first added to the water, mixed for 1 min, and poured into plastic matrix molds, in order to form the plaster molds. After hardening the mold, it was removed and dried at room temperature for 15 days before use and characterization tests. The molds were produced in rectangular format, measuring 8 cm in length and 10 cm in width. The slate powder was collected in the Pompéu region (Minas Gerais, Brazil), in a processing plant. The suspensions of slate powder in distilled water were prepared with a constant solid content (65% w/w) and homogenized with a magnetic stirrer for 24 h. The dispersant used was ammonium polyacrylate (1% w/w, Sigma Aldrich).

Particle size distribution was measured using a granulometer (mod. 1090, Cilas) applying Fraunhofer's theory. In order to identify the mineralogical composition, X-ray diffraction (XRD) tests were carried out in a diffractometer (PW1730/10, Philips) with $\text{CuK}\alpha$ radiation, 35 kV, goniometer speed of $0.02^\circ/\text{min}$ with a time count of 5 s/step and collected from 5° to 80° in 2θ . The XRD pattern interpretations were performed by comparison with the standards contained in the PDF database 02 (ICDD, 2013). For the refinement, the General Structure Analysis System Program [7] was used with the EXPGUI interface using the Thompson-Cox-Hastings pseudo-Voigt profile function, with background radiation adjusted by the Chebyshev polynomial. The values for R_p , R_{wp} , and χ^2 were measured to check the quality of the refinement. The chemical composition (semi-quantitative analysis) of the powders was obtained by X-ray fluorescence spectroscopy (XRF), performed with a spectrometer (EDX-720, Shimadzu) in

vacuum. The particle density was measured by means of a helium pycnometer (AccuPyc 1330, Micromeritics).

After casting, the pieces were dried at room temperature for 24 h, followed by oven heating at 105°C and finally heat-treated in an electric oven until 1050°C in the air with a heating rate of $10^\circ\text{C}/\text{min}$. The samples (ceramic pieces and plaster molds) were characterized through a scanning electron microscope (SEM, SSX-550, Shimadzu), with a secondary electron detector operating at 15 kV. The SEM images were used to determine the porosity via image analysis using ImageJ software. The program identified pixels with intensities that comprised values ranging from 0 (as black as possible) to 255 (as white as possible), representing a range of 256 shades of grey. It determined the accumulated histogram of a certain grey range of the image and assumed the inflection point of the histogram profile curve. This point represented the grey value used as the separation threshold for various regions of the image. From threshold determination, the program checked all the pixels in the image, selecting those with intensities whose values were below or equal to the threshold value. The sum of all pixels, measuring the area below the curve, allowed the estimation of their proportion in relation to the total image area, providing the porosity percentage [8]. For this paper, five images of random regions of each specimen were analyzed by two different operators. The final porosity value was defined as the mean of the analysis. The standard deviation was also calculated. The physical properties (water absorption, porosity, density, impermeable pores) were evaluated following the ASTM C373-17 standard [9]. Mechanical rupture tests were performed according to procedures recommended by NBR 12129-17 standard [10] for plaster samples and NBR 15270-1:2017 standard [11] (adapted) for ceramic slate pieces. The adaptation may be justified because the slate pieces can be framed in a group of traditional red ceramic materials. The tests were performed at room temperature with a universal mechanical testing machine (Autograph AG-X, Shimadzu).

RESULTS AND DISCUSSION

Raw materials

Fig. 1 shows the particle size distribution curves for the gypsum and slate powders, obtained by a laser diffraction (LD) method. The curve for gypsum powder was approximately monomodal, with particle sizes ranging from 0.1 to $224\ \mu\text{m}$, with the main peak at $20\ \mu\text{m}$ and a small peak at $0.5\ \mu\text{m}$ (Fig. 1a). The highest value of particle size, more than $100\ \mu\text{m}$, suggested the presence of particle clusters. In Fig. 1b, it can be noticed that the curve for slate was likewise close to monomodal. The slate powder sample had a major peak at a considerably large size, closer to $5\ \mu\text{m}$, and a secondary peak close to $1\ \mu\text{m}$. Table I presents the specific particle diameters for the plaster (gypsum) and slate powders.

It is fundamental to determine the particle size, as it

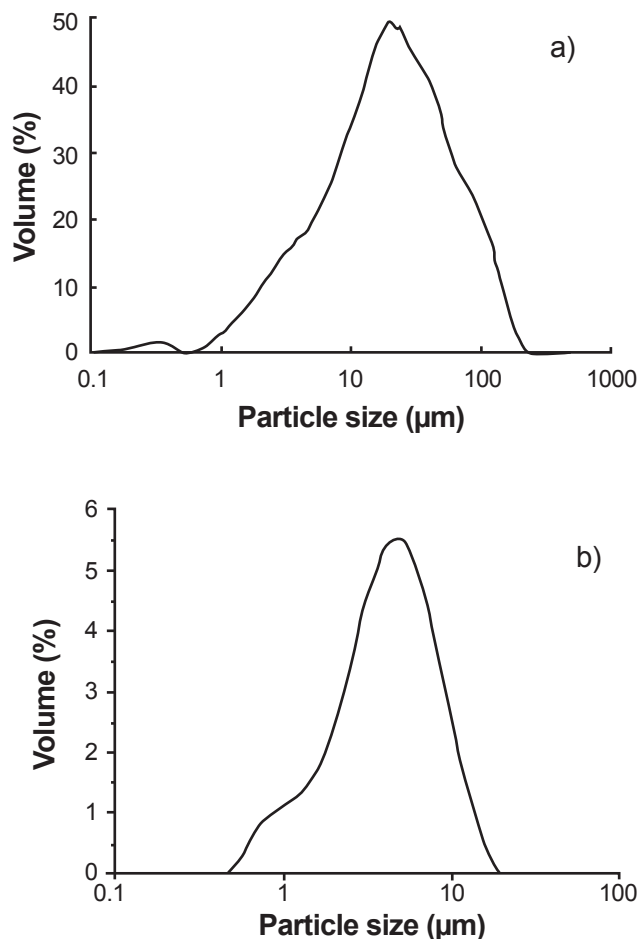


Figure 1: Particle size distribution curves for gypsum powder (a) and slate powder (b).

Table I - Particle size distribution data (μm) of gypsum and slate powders.

Powder	d(0.1)	d(0.5)	d(0.9)
Gypsum	3.16	18.93	75.82
Slate	0.89	6.77	24.81

influences the reaction kinetics. The hydration rate increases with decreasing particle size and with the increase of plaster's specific surface area. Fig. 2 shows the SEM image obtained for the gypsum powder. There was a wide range of variation in particle sizes with values between 5 and 100 μm. Using a scanning electron microscope, randomly chosen particles had their sizes measured and the average value found was 16.9 μm. According to Singh and Middendorf [12], SEM images have shown that the α-hemihydrate consists of well-formed transparent idiomorphic crystals with sharp crystal edges, whereas β-hemihydrate consists of flaky particles made up of small crystals as observed in Fig. 2. β-hemihydrate requires more water than the α-hemihydrate in order to obtain a paste of workable consistency as it has a much higher specific surface area, which provides more nucleation sites for the gypsum crystallization.

Table II shows the results of semiquantitative chemical

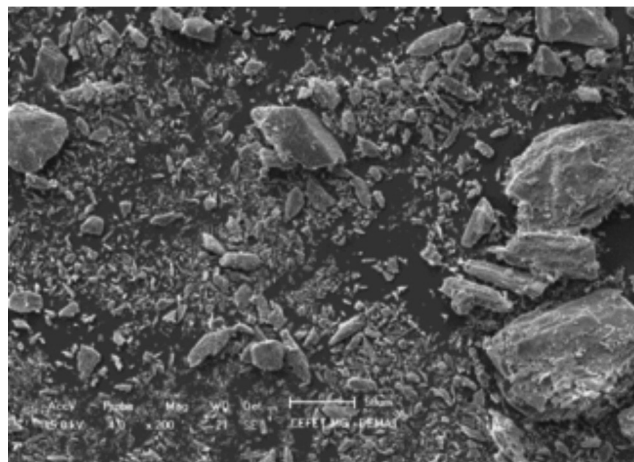


Figure 2: SEM image of gypsum particles.

analysis of the plaster obtained by X-ray fluorescence spectroscopy (XRF). The analysis presented the values of the elements in mass percentage. The presence of calcium, sulfur, and oxygen referred to the calcium sulfate's chemical composition, hinting at the high purity of the raw material, along with the presence of small traces of P and Fe. Yu and Brouwers [13], when studying the microstructure and mechanical properties of β-hemihydrate, found similar chemical composition values: O=46.86%, Ca=26.68%, S=21.46%. According to them, there were merely small impurities in the sample (Si, Mg, and Al less than 3% of total mass), and the amounts of Ca and S were in line with the theoretical values, which was also confirmed by the XRD result. Barbosa *et al.* [2] obtained similar results working with plaster of Paris in Brazil (O=45.0%, Ca=33.2%, S=21.1%). The results of XRF analysis (Table II) indicated abundant contents of SiO₂, Al₂O₃, and Fe₂O₃ in the slate powder; all three oxides were the major constituents. Catarino *et al.* [14] found similar values using the XRF chemical analysis, which indicated the presence of 54.68% SiO₂, 9.95% Fe₂O₃, and 23.52% Al₂O₃. According to Cambronerio *et al.* [15], the slate powder's chemical composition consists mainly of SiO₂ (50-60%) and Al₂O₃ (20-25%). The powder's XRD tests have shown peaks corresponding to the following constituents: quartz, hematite, chlorite, and muscovite.

The use of X-ray powder diffraction, combined with Rietveld refinement, is widespread in the literature for the quantification of the phases present in materials from different areas. However, in gypsum or plaster studies, the XRD technique is used, in general, to qualitatively determine the phases present in the material. Still, there are few studies employing the Rietveld method to perform quantitative phase analyses (QPA), such as the one performed elsewhere [16]. The researchers used the QPA combined with XRD data and determined a basanite content equal to 99.80% in a sample of recycled gypsum plasterboard. Cordon *et al.* [17] compared a recycled gypsum waste with a commercial plaster, expecting to find only the main sulfate compounds (basanite and anhydrite), but as the origin of commercial plaster was not known, they ended up finding impurities

Table II - Semiquantitative analysis by XRF (mass%) for the gypsum and slate powders.

Powder	SiO ₂	Al ₂ O ₃	Fe ₂ O ₃	K ₂ O	CaO	MgO	SO ₃	P ₂ O ₅
Slate	61.6	16.6	5.9	10.8	2.6	2.5	-	-
Gypsum	-	-	0.9	-	46.9	-	50.8	1.4

(mainly carbonates), such as dolomite and calcite, among others. According to Seufert *et al.* [18], samples with low contents of anhydrite III and basanite require fixing of the basanite lattice parameters to stabilize the quantification results. All samples studied by them consisted of at least two calcium sulfate phases with different reactivity rates.

We, conversely, laid XRD data to perform some Rietveld refinement and the software Crystallographica Search-Match (integrated to a PDF2 database, distributed by the International Centre for Diffraction Data) and QualX2, using a built-in version of the Crystallography Open Database in order to gather the required structural information. Fig. 3a demonstrates a peak relative to basanite (CaSO₄·½H₂O) and anhydrite (CaSO₄). Basanite was the main mineral phase identified, with 75.3%, and anhydrite with 24.7%. The anhydrite is a subproduct of the calcination process. Gholami and Khakpour [19] affirmed that β-hemihydrate calcium sulfate and the α-hemihydrate present similar XRD patterns, with almost identical peak positions. However, β-hemihydrate shows a smaller crystallite size, which results in lower and broader peaks in terms of the XRD pattern when compared to α-hemihydrate. This may advocate that the XRD pattern of gypsum in Fig. 3a is β-hemihydrate, according to SEM analysis. Another study [20] found similar phases in gypsum powders. The gypsum density was found via helium pycnometer and the value was 2.83 g.cm⁻³.

The chemical analysis of a slate powder used to produce the ceramic pieces depends on the region where it was extracted, but in general, the oxides of silicon, aluminum, iron, and others are witnessed in smaller amounts. The presence of large amounts of silicon and aluminum oxides could be observed due to the presence of silico-aluminous minerals in the slate samples. Despite the different regions where slate has been studied (Brazil, Portugal, and Spain), several authors have shown similar results with silicon oxide contents varying from 55-61%, aluminum oxide from 18-24%, and iron oxide from 7-10%. In addition, the slate powder's density and surface area were, respectively, 2.76 g.cm⁻³ and 15.8 m².g⁻¹. Fig. 3b shows a typical diffractogram for the slate powder. By analyzing the obtained diffraction pattern, the following minerals were identified: quartz (SiO₂), clinocllore, muscovite, albite, hematite, and orthoclase. The slate powder's mineralogical analysis, shown in Table III, was obtained through refinement by the Rietveld method. The refinement quality was verified through numerical statistical parameters R_p (profile factor), R_{wp} (weighted profile factor), and χ² (goodness of fit, GOF, S). The adjustment parameters R_p and R_{wp} for the analyzed samples were, respectively, 5.3 and 7.3. Some samples of Brazilian slates were analyzed and values similar to this

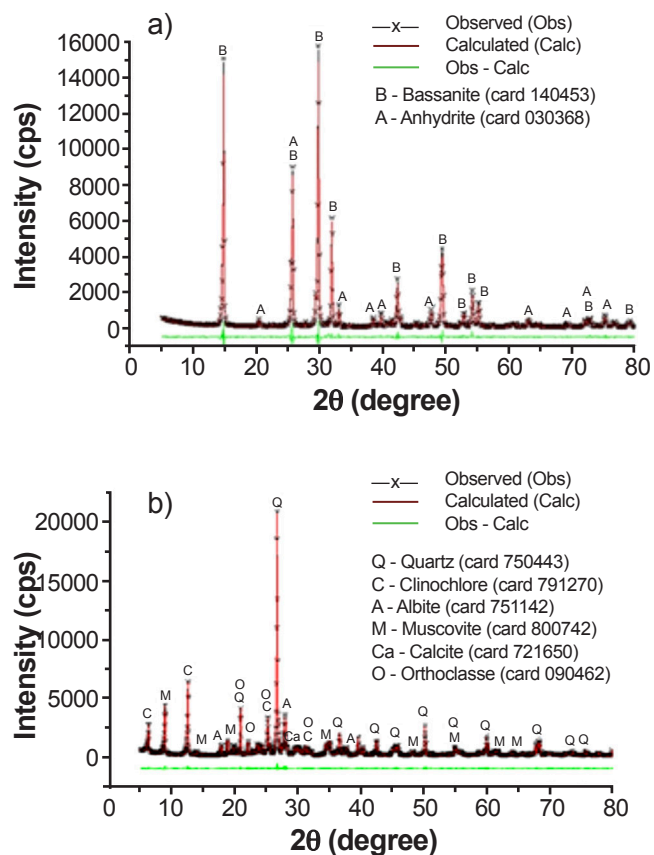


Figure 3: X-ray diffractograms with Rietveld refinement for gypsum powder (a) and slate powder (b).

work were found [21]; the values were 26-30% of quartz, 32-34% mica, 18-20% chlorite, 12-15% feldspar, and 0.5-1% carbonates. Campus [22] studied seven slate samples from different places in Spain, aiming their application in alkali-activated reactions in cement and mortar. It was demonstrated that all tested slates were susceptible to alkali-silica and alkali-silicate reactivity with cement alkalis. The analyzed samples presented the following compositions: 10-35% quartz, 25-65% muscovite, 2-19% clinocllore, and others, such as calcite, hematite, rutile, and pyrite, in smaller quantities.

In their study, Ward and Gomez-Fernandez [23] worked with slates from two mines and used them on roofs, which showed a high level of consistency between the values of the oxide percentages obtained by QPA inferred from the XRD study and the equivalent oxide proportions determined by direct chemical analysis. A total of 24 samples from the Iberian Massif in North-Western Spain were analyzed and the results exhibited the following compositions: 19-42.8% quartz, 29.6-56.5% muscovite, 11.4-34% clinocllore,

Table III - Results of mineralogical analysis (mass %) of the slate powder from Minas Gerais, Brazil.

Quartz	Albite	Clinochlore	Muscovite	Orthoclase	Calcite
51.9	15.1	13.7	11.1	6.9	1.3

1.6-24.5% albite, 0.1-3.6% rutile, and others in smaller quantities, such as talc, paragonite, and anatase. Comparing the obtained results from chemical and mineralogical analyses, it was observed that generally, silica (SiO_2) is the dominant oxide, contained in quartz, phyllosilicates (micas and chlorites), and plagioclases (feldspars). Alumina (Al_2O_3) is mainly contained in phyllosilicates and, to a lesser extent, in feldspars, the same way as sodium and potassium oxides. Part of the potassium is present in muscovite, and the magnesium oxide makes up the clinochlore and the magnesian calcite.

Hydrating system microstructure

The general plaster mold microstructure and fragile fracture surface are shown in Fig. 4. It was prepared with a P/W ratio of 70. The structure exemplifies a set of plaster crystals formed by prismatic needle clusters, whereas the dark regions between the needles are empty spaces, or pores, similar to the example studied by Coquard *et al.* [24] with 57.7% porosity. According to them, experiments carried out with solid particles on less concentrated solutions formed heterogeneous nucleation, in which the process appeared to be faster in the hemihydrate paste, inducing the occurrence of smaller gypsum needles.

SEM images showing the morphology of each plaster prepared with different P/W ratios are shown in Fig. 5. From Figs. 5a to 5d, as the P/W ratio increased, the pores also dilated, due to the remaining water from the gypsum powder's hydration process. When the quantity of water is higher than the stoichiometric value for hydration, the volume of water that does not react forms pores after drying. Therefore, it can be deduced that the P/W ratio has a linear relationship with porosity and percentage of water absorption; this was also observed by Wahab *et al.* [25]. In all images, a heterogeneous aspect was observed with crystal needle agglomerates of different sizes, along with the presence of randomly distributed pores of different sizes. The effect of plaster mold preparation variables was evaluated by Ochoa *et al.* [26]; they observed needle-like structures in all samples, but, according to them, the longer the stirring time, the narrower was the gypsum crystals, and the higher the water temperature used, the larger was the gypsum crystals formed. However, the medium pore diameter of the plaster molds was not affected and the value found for both cases was 3.34 μm .

The P/W ratio influences the precipitation rate of the dihydrate crystals, which grow from crystallization germs or nuclei. The number of nuclei in the solution influences the growth rate and size of the crystals. When the nuclei are numerous, the growth is fast and there is the formation of small

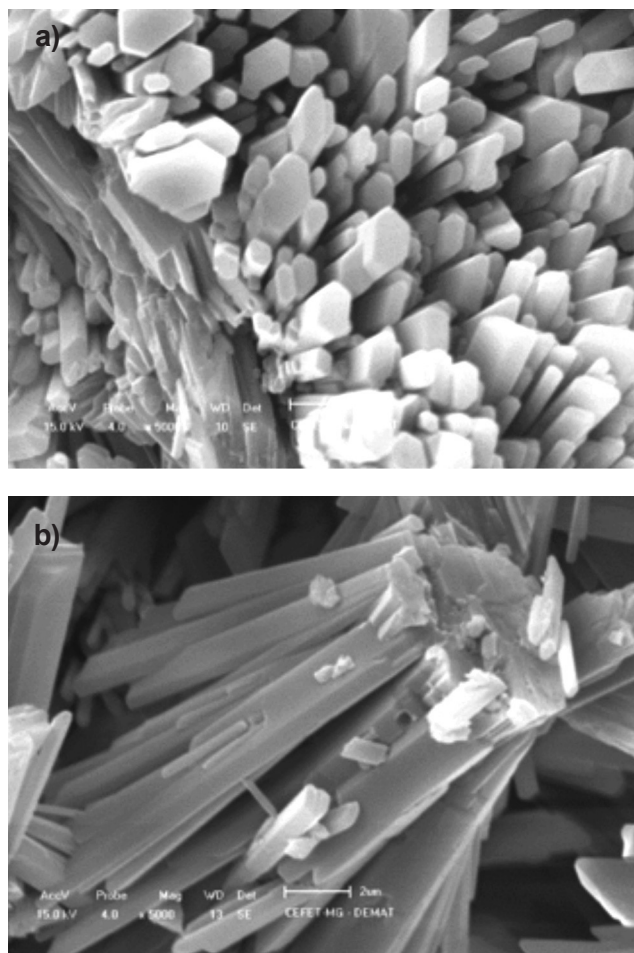


Figure 4: SEM images of typical gypsum showing the prismatic crystal needles (a) and a fragile fracture of a plaster mold (b).

crystals per volume unit of the solution. When few nuclei are formed, the growth is slow, which favors the formation of large crystals [27]. Microstructures formed of large crystals (Fig. 5d) are less resistant (more porous) than those formed by small (denser) crystals (Fig. 5a). From the SEM images, it is clear that the crystals in Fig. 5a are much tighter and more homogeneous than that in Fig. 5d. This showed that the plaster produced with lower water proportion provided better bonding between the gypsum crystals, which should designate better mechanical properties. Several attempts have been made to quantify the mechanical properties of plaster as a function of porosity for different uses. In slip casting, the fabrication and design of the plaster molds are so vital because the casting rate depends on the balance between plaster mold suction and transferability of both piece and mold. Therefore, it is necessary to use adequate P/W ratios, which in turn lead to higher mechanical strength to handling the mold and appropriated porosity. Any change in porosity leads to changes in casting rate and the final properties of the produced pieces. Gholami and Khakpour [19] using a retardant (melamine-formaldehyde sulfonate) obtained adequate fluidity to produce molds with high P/W ratios, reducing the porosity and consequently the casting rate to obtain high green density.

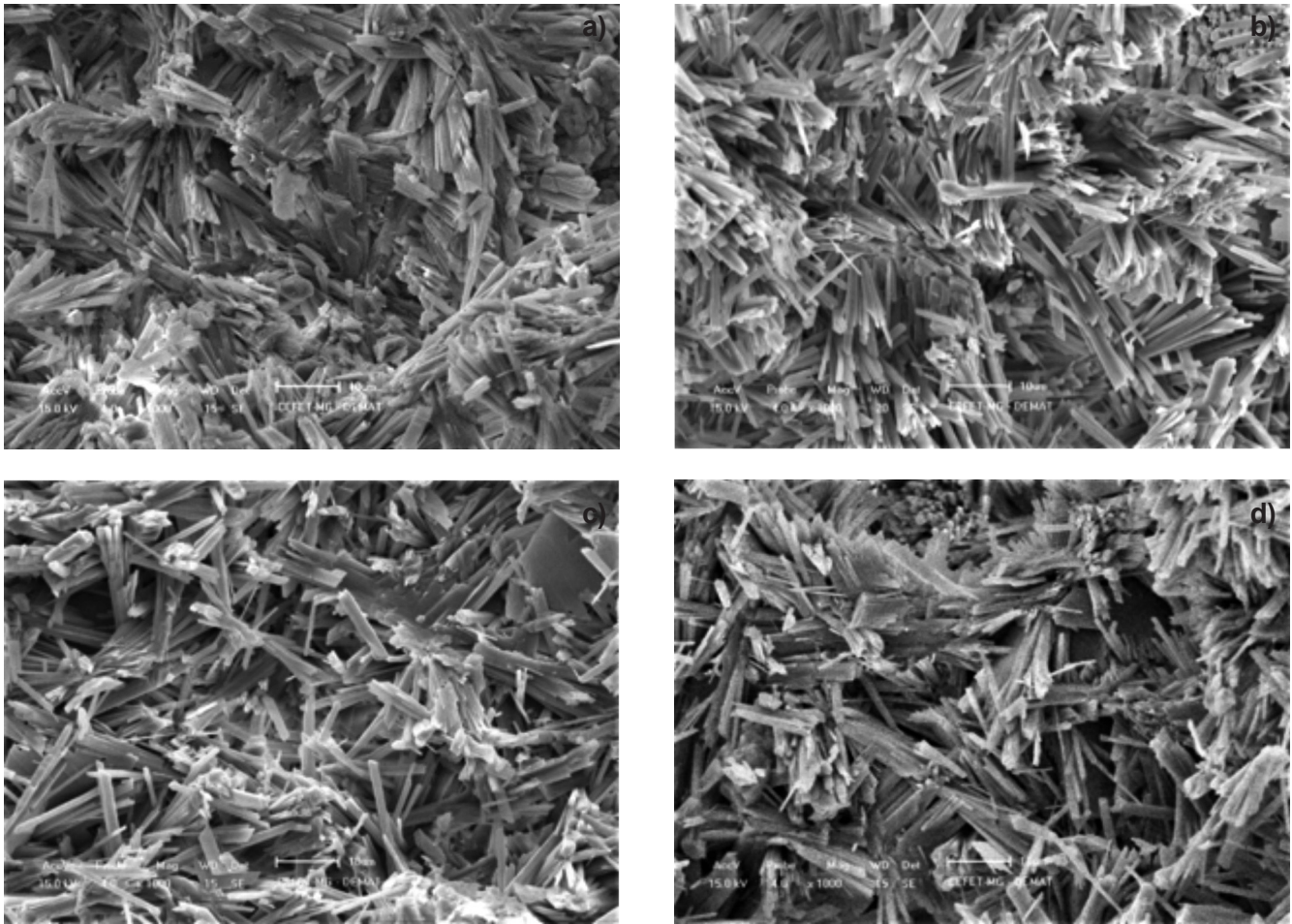


Figure 5: SEM images of the plaster produced with P/W ratio of: a) 50; b) 60; c) 70; and d) 80.

The results obtained for porosity by image analysis and the geometric method are shown in Table IV. The image analysis process is a swift procedure to quantify the porosity, however, the effectiveness of the study depends on some factors, such as the magnification capacity of the microscope and view area, as well as the number of images to be analyzed and the program operator in the definition of the threshold. The differences between the values obtained were due to the different methodologies adopted in each test. It was observed that for greater consistencies (higher water content) there was a gradual increase in porosity for the two techniques used. The porosity of the dihydrate is related to the rate of nucleation (where crystallization begins) since the formation of large clusters with irregular shapes provides less compaction of the crystals. The greater the amount of water used to hydrate the powder, the greater shall be the number of pores left after curing the block, which corroborates with the micrographs shown in Figs. 5a to 5d. The porosity and water absorption of the mold are related to the remaining water from the hydration process of the gypsum powder, an occurrence that is due to the use of a higher quantity of water than the stoichiometric value for the hemihydrate's hydration. Thus, the quantity of water that does not react with the powder occupies volume between

the crystals, and after curing the dihydrate, the water evaporates, leaving voids in the material. Density values of approximately 1.9, 1.0, and 0.84 g/cm³ for the consistencies of 50, 70, and 90, respectively, were obtained by Farias *et al.* [28], and density values of 1.15, 1.04, and 0.96 g/cm³ for 60, 70, and 80 consistencies, respectively, were found by Wiss *et al.* [29].

Fig. 6 shows a graph with the values of compressive strength and flexural strength for the four studied consistencies. It is often reported that the ratio of variation in the plaster/water ratio affects the flexural and compressive mechanical properties of gypsum molds. Campus [22] found flexural strength values of 1.3, 3.8, and 6.8 MPa for consistencies of 70, 60, and 50, respectively. Yu and Brouwers [13] demonstrated flexural strength values of 5.8 and 3.1 MPa and compressive strength of 14.1 and 8.9 MPa, respectively, for consistencies of 50 and 60. According to Wiss *et al.* [29], the compressive strength values for consistencies of 60, 70, and 80 were 16.6, 12.4, and 8.9 MPa, respectively. Farias *et al.* [28] studying Brazilian plasters found compressive strength values of 4.8, 1.7, and 1.1 MPa, respectively, for the consistencies of 50, 70, and 90. The differences between the values obtained can be explained by the different sizes of non-standardized samples. In their

Table IV - Results of porosity, bulk density, and pore volume obtained by geometric method and porosity by image analysis.

Plaster/ water ratio	Bulk density (g/cm ³)	Porosity (%)	Porosity (%)	Pore volume (mL/g)
2.00	1.4±0.1	34.3±0.1	19.9±0.3	0.285±0.010
1.67	1.2±0.1	41.4±0.1	33.6±0.3	0.389±0.010
1.43	1.1±0.1	47.1±0.1	41.1±0.3	0.520±0.010
1.25	0.9±0.1	51.9±0.1	45.1±0.3	0.860±0.010

work, Coquard *et al.* [30] showed that sample size influences mechanical strength values. They systematically observed that small samples exhibit greater strength than large samples. According to Farias *et al.* [28], Wiss *et al.* [29], and Coquard *et al.* [30], as the amount of water increases, the fraction of voids (porosity) between the crystals in the mold also increases, weakening the connections between the crystalline structure of the dehydrated gypsum, affecting the mechanical strength of the mold; in Fig. 6, it was observed that as the P/W ratio increased, the flexural and compressive strengths decreased.

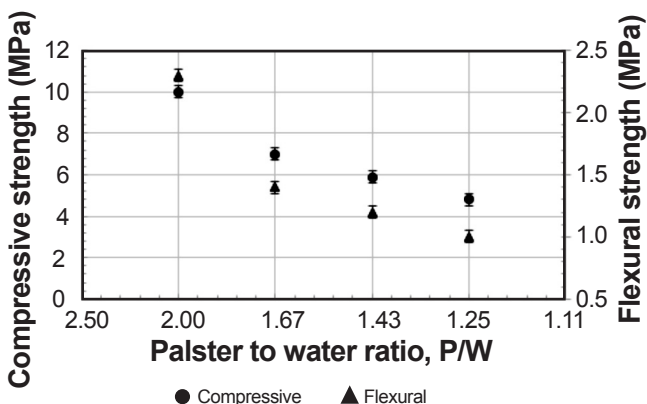


Figure 6: Mechanical properties of plaster molds.

Slate pieces' microstructure

The slate powder suspension was poured into plaster molds with different consistencies, and the casting rate on the mold surface was measured at two values of pH, 8.36 (natural pH of the suspension) and 10, adjusted with NaOH solution (0.1 mol/L). Table V shows the results obtained for the casting rate at the two pH values. According to Palhares [31], slate suspensions are more stable at higher pH, when a greater distribution of negative charges is achieved on the particle surfaces of the different constituents of the slate, promoting better repulsion. It was observed that the greater the consistency of the plaster mold, the greater the casting rate on its surface. This fact can be explained by the greater volume of pores contained in the mold structures that present greater water suction force in their capillaries, leading to the consolidation of a larger amount of particles during the slip casting process. When comparing the casting rates for the

two studied pHs, it was observed that at pH 10 the casting rate decreased. The increase in the pH of the suspension favored the formation of negative charges on the edges of the particles, helping to deflocculate the system. As a result, the ceramic suspension was more stable, that is, there was a greater repulsive interaction produced in a more efficient manner due to electrostatic repulsion and steric stabilization. As a result, higher densities of ceramic tiles were observed due to better compaction.

Table V - Casting rate for different plaster/water ratios of molds.

Plaster/water ratio	Casting rate (mm/min)	
	pH 8.36	pH 10
2.00	2.40±0.01	2.05±0.01
1.67	2.55±0.01	2.15±0.01
1.43	2.60±0.01	2.25±0.01
1.25	2.65±0.01	2.30±0.01

According to the research developed by Coquard *et al.* [30] on the process of slip casting slate suspension using molds with a P/W ratio of 70, it is possible to emphasize that the diversity of slate composition, due to its difference in structural components, according to the location of its extraction, can result in different values of casting rate. The increase in the P/W ratio leads to the production of more porous molds and these, consequently, have greater water absorption capacity; when used in the slip casting process, they act as filtering agents for the water present in the suspension, causing the resulting ceramic piece to have less water in its structure and therefore less porosity. The lowest density values presented in Table VI were found for parts produced by molds with consistency 50, which presented the highest pore volumes in their structures. The samples of consistency 80, on the other hand, exhibited the highest density values, as they presented the final pieces with the least amount of pores since these molds had a high capacity for absorbing water present in the suspension. Regarding the effect of the pH variation of the ceramic suspensions, it can be said that for all plaster molds and consistency variations, the porosity values were lower for pieces produced with ceramic suspension with pH 10. As shown in the results of slip casting (Table V), ceramic suspensions with pH 10 required more time to promote particle consolidation, due

Table VI - Porosity and bulk density for different plaster/water ratios of molds and pH of slate suspensions.

Plaster/water ratio	Porosity (%)		Bulk density (g/cm ³)	
	pH 8.36	pH 10	pH 8.36	pH 10
2.00	32.4±0.1	17.2±0.1	1.8±0.1	2.2±0.1
1.67	30.4±0.1	16.5±0.1	1.7±0.1	2.1±0.1
1.43	26.7±0.1	14.6±0.1	2.1±0.1	2.2±0.1
1.25	25.1±0.1	9.8±0.1	2.1±0.1	2.5±0.1

to the greater spacing between the particles dispersed in the fluid medium. This greater distance between the particles, combined with the longer consolidation time, may promote a more efficient packaging and lead to a decrease in the material structure's pore volume.

The lowest density values, presented in Table VI, were found for the pieces produced by molds with the consistency of 50, which presented the largest pore volumes in their structures. Consistency 80 samples, on the other hand, exhibited the highest values of bulk density, as they had the final parts with the lowest pore quantity. As density is inversely related to the pore volume of the material, where higher density values are obtained for more compact parts, it is possible to explain the lower density values for suspensions produced with pH 8.36, because more porous ceramic pieces were obtained at this pH rate. The analysis of the slate ceramic suspension's pH variation showed a significant difference in the results obtained for all tests performed (porosity, water absorption, and density). It was observed that with the increase of the pH to 10, the values obtained were better due to the greater stability of the slate suspension, thus being of fundamental importance to the study of the pH for projects involving the slip casting process. Density values before and after heat treatment were 2.4 and 2.2 g/cm³, respectively; values found by Palhares and Mansur [32] are higher due to the addition of a binder, polyvinyl alcohol, which promoted the formation of bridges between the particles, improving compaction and increasing density. According to them, the decrease in density after heat treatment is due to the phase transformations that the clinocllore and muscovite constituents undergo when heated. Both have their crystalline structures transformed, their volumes increased, and pieces' densities decreased. The effect of variation in porosity and density of ceramic pieces produced by slip casting using two types of gypsum, β - and α -gypsum, and β -gypsum with melamine-formaldehyde sulfonate (MFS) as a retarder was studied [19]. The authors concluded that the greater the amount of water in the plaster mold, the smaller the porosity of the pieces and, consequently, the greater the density.

CONCLUSIONS

This work demonstrated that the slip casting process using plaster molds allowed the production of ceramic slate pieces. Yet, it is worth mentioning that the parameters that influence slip stability and the quality of plaster molds must

be observed in order to optimize the process. Regarding the molds, the higher the plaster/water ratio, the greater the porosity and lower the density. It was exposed that these characteristics influence the properties of the produced slate pieces and that by increasing the plaster/water ratio, there is a meaningful porosity decrease and an increase in their densities. As the bonding process resembles a filtration, in the case studied, the casting rate on the surface of plaster molds increased with consistency. However, it is known that total porosity is not the only factor that influences this property, but also the pore size distribution in the mold. In view of what was presented, it can be concluded that the increase in the plaster/water ratio employed in the preparation of the samples generated a crystalline network with less mechanically resistant and larger crystals, due to the porosity increase of the material. The comparison of green and heat-treated parts showed a reduction in porosity with treatment at temperatures of approximately 1050 °C. This porosity probably can be further reduced by increasing the heat treatment temperatures, which can lead to the partial melting of constituents of the slate, forming a liquid phase and filling the pores.

REFERENCES

- [1] J. Catafesta, R. Andreola, C.A. Perottoni, J.E. Zorzi, *Cerâmica* **53**, 325 (2007) 29.
- [2] A.A. Barbosa, A.V. Ferraz, G.A. Santos, *Cerâmica* **60**, 356 (2014) 501.
- [3] L.B. Palhares, H.S. Mansur, in Proc. 13th Brazil. Congr. Mater. Eng. Sci., Curitiba (1998) 3430.
- [4] G. Vekinis, M.F. Ashby, P.W.R. Beaumont, *J. Mater. Sci.* **28** (1993) 3221.
- [5] C.E.G. Ribeiro, J.S.R. Rubén, E.A. Carvalho, *Constr. Build. Mater.* **149** (2017) 149.
- [6] C. Chiodi Filho, "Balance of Brazilian exports and imports of ornamental stones", Abirochas, S. Paulo (2018).
- [7] A.C. Larson, R.B. Von Dreele, "General structure analysis system (GSAS)", Rep. LAUR 86-748, Los Alamos National Laboratory (2001).
- [8] S.L. Correia, B.W. Matos, G. Santos, A. Dezanet, D. Stringari, A. Schackow, A.M. Segadães, in Proc. 21st Brazil. Congr. Mater. Sci. Eng., Cuiabá (2014) 478.
- [9] ASTM C373, "Glass and ceramic", Am. Soc. Test. Mater. (2017).
- [10] NBR-12129, "Plaster for civil construction: determination of mechanical properties", Brazil. Ass. Techn.

Stand. (2017).

[11] NBR-15270-1 “Ceramic components: blocks and bricks for masonry, part 1: requirements”, Brazil. Ass. Techn. Stand. (2017).

[12] N.B. Singh, B. Middendorf, *Prog. Cryst. Growth Charact. Mater.* **53** (2007) 57.

[13] Q.L. Yu, H.J.H. Brouwers, *Constr. Build. Mater.* **25** (2011) 3149.

[14] L. Catarino, J. Sousa, I.M. Martins, M.T. Vieira, M.M. Oliveira, *J. Mat. Proc. Tech.* **143-144** (2003) 843.

[15] L.E.F. Cambroner, J.M. Ruiz-Roman, J.M. Ruiz-Pietro, *Bol. Soc. Esp. Ceram. V.* **44**, 6 (2005) 368.

[16] A. Ahmed, K. Ugai, T. Kamei, *Constr. Build. Mater.* **25** (2011) 208.

[17] H.C.F. Cordon, F.C. Cagnonia, F.F. Ferreira, Brazil. *J. Build. Eng.* **22** (2019) 504.

[18] S. Seufert, C. Hesse, F. Goetz-Neunhoeffler, J. Neubauer, *Cem. Concr. Res.* **39** (2009) 936.

[19] M. Gholami, Z. Khakpour, *J. Aust. Ceram. Soc.* **55** (2018) 633.

[20] M. Lanzón, P.A. García-Ruiz, *Constr. Build. Mater.* **28** (2012) 506.

[21] C. Chiodi Filho, E.P. Rodrigues, A.C. Artur, *Rev. Geocic.* **22**, 2 (2003) 119.

[22] P.L. Campus, *Est. Geol.* **66** (2010) 91.

[23] C. Ward, F. Gomez-Fernandez, *Eur. J. Mineral.* **15** (2003) 1051.

[24] P. Coquard, R. Boistelle, L. Amathieu, P. Barriac, *J. Mater. Sci.* **29** (1994) 4611.

[25] N.H.A. Wahab, N.H. Saad, A.R.M. Sahab, N. Nasir, A.A. Rashid, *Sci. Int.* **29**, 4 (2017) 843.

[26] R.E. Ochoa, C.A. Gutiérrez, J.C. Rendón, J.L. Rodríguez, *Bol. Soc. Esp. Ceram. V.* **56** (2017) 263.

[27] R.P.N. Antunes, “Study of the influence of hydrated lime on plaster pastes”, M.Sc. Diss., S. Paulo Un. (1999).

[28] G.M. Farias, A.V. Ferraz, A.L.M. De Souza, P.G. Da Costa, *Evolvere Sci.* **3**, 1 (2014) 107.

[29] J.E. Wiss, T.P. Camp, R.B. Ladoo, in *Annual Meet., Am. Ceram. Soc., Westerville* (1930) 287.

[30] P. Coquard, R. Boistelle, *Int. J. Rock Mech. Min. Sci.* **31**, 5 (1994) 517.

[31] L.B. Palhares, “Study of the stability and behavior of aqueous slate powder suspensions for application in ceramic processing”, PhD Thesis, Fed. Un. Ouro Preto (2017).

[32] L.B. Palhares, H.S. Mansur, in *Proc. 15th Brazil. Congr. Mater. Sci. Eng., Natal* (2002) 1211.

(*Rec. 26/07/2021, Rev. 01/09/2021, 01/10/2021, Ac. 03/11/2021*)

